Combined Vis and NIR imaging | Hot Paper

DOI: 10.1002/ange.201311028

Polynuclear Sm^{III} Polyamidoamine-Based Dendrimer: A Single Probe for Combined Visible and Near-Infrared Live-Cell Imaging**

Alexandra Foucault-Collet, Chad M. Shade, Iuliia Nazarenko, Stéphane Petoud, and Svetlana V. Eliseeva**

Abstract: *We report herein the synthesis of a luminescent polynuclear dendritic structure (Sm^{III}-G3P-2,3Nap) in which eight Sm^{III} ions are sensitized by thirty-two 2,3-naphthalimide chromophores. Upon a single excitation wavelength, the dendrimer complex exhibits two types of emission in the visible and in the near-infrared (NIR) ranges. Sm^{III}-G3P-2,3Nap was non-cytotoxic after 24 h of incubation and up to 2.5 μM. The ability of the Sm^{III}-based probe to be taken up by cells was confirmed by confocal microscopy. Epifluorescence microscopy validated Sm^{III}-G3P-2,3Nap as a versatile probe, capable of performing interchangeably in the visible or NIR for live-cell imaging. As both emissions are obtained from a single complex, the cytotoxicity and biodistribution are inherently the same. The possibility for discriminating the sharp Sm^{III} signals from autofluorescence in two spectral ranges increases the reliability of analysis and reduces the probability of artifacts and instrumental errors.*

The high sensitivity of fluorescence-based imaging techniques enables the real-time study of biological entities or specific targets in cellulo and in vivo, translating into advanced clinical awareness for a large number of diseases and improved treatment plans. The challenge which limits widespread implementation of fluorescence imaging is the intrinsic fluorescence of biomolecules that interferes with the emission signal arising from the targeted bioprobes.[1] Thus, the design of bioprobes with excitation and emission wavelengths that avoids the pitfalls of autofluorescence, a biological window between 650–900 nm, has received a considerable interest.[2] Special attention has been received by Ln^{III}-based probes,[3] since they offer several complementary advantages, including: 1) characteristically sharp emission bands which collectively span the visible and NIR ranges, 2) their spectral positions are insensitive to changes in the local microenvironment (such as pH value and temperature), 3) large energy separation and thus little-to-no spectral overlap between emission and excitation wavelengths, and 4) improved resistance to photobleaching. Among the Ln^{III} ions, Sm^{III} has rich spectroscopic properties as a result of electronic transitions that originate from the $^4G_{5/2}$ energy level, producing sharp bands in the visible ($^4G_{5/2}\rightarrow{}^6H_J$) and in the NIR ($^4G_{5/2}\rightarrow{}^6F_J$) ranges.[4] Organic ligands have been designed[5] and Sm^{III}-based visible emitting bioprobes have been successfully used in different homo- and heterogeneous assays.[6] However, only one example of cell imaging using a Sm^{III}-based bioprobe is reported to date and only the visible-emitting properties have been exploited.[7] Since their synthetic development,[8] dendritic polymers have gained momentum in different applications ranging from catalysis and materials/environmental sciences to biology and nanomedicine.[9] In particular, polyamidoamine dendrimers have demonstrated considerable potential as drug/DNA/amino acid delivery systems or, once decorated with appropriate functional entities, as probes for magnetic resonance, fluorescence or γ-ray imaging.[10] However, reports taking advantage of polyamidoamine dendrimers and their derivatives for the protection and sensitization of Ln^{III} ions remain scarce.[11]

We have previously reported that all thirty-two terminal amino groups of a generation-3 polyamidoamine dendrimer can be covalently substituted by naphthalimide chromophores, including 4-amino-1,8-naphthalimide (G3P-4A1,8Nap)[12] and 2,3-naphthalimide (G3P-2,3Nap).[11d] These functionalized dendrimers can incorporate eight lanthanide ions inside their branches, forming robust luminescent probes with optimized intensity due to the combination of a large number of chromophoric groups and Ln^{III} ions within a discrete macromolecule. The fast intersystem crossing within the 2,3-naphthalimide group ($k_{isc}=8.5\times10^7\ s^{-1}$) and, consequently, the high population of the triplet state located at an energy position favorable for the sensitization of Sm^{III} ions (20280 cm^{-1}) makes this chromophore a wise choice for the design of luminescent probes. Herein, we take advantage of the combined properties of G3P-2,3Nap dendrimers and Sm^{III} ions with an ultimate goal of creating a single bioprobe suitable for live-cell imaging in either the

[*] Dr. A. Foucault-Collet, I. Nazarenko, Prof. Dr. S. Petoud, Dr. S. V. Eliseeva
Centre de Biophysique Moléculaire, CNRS UPR 4301
Rue Charles Sadron, 45071 Orléans (France)
E-mail: stephane.petoud@inserm.fr
Dr. C. M. Shade, Prof. Dr. S. Petoud
Department of Chemistry, University of Pittsburgh
Pittsburgh, PA 15260 (USA)
Dr. S. V. Eliseeva
Le Studium, Loire Valley Institute for Advanced Studies, 1 Rue Dupanloup, 45000 Orléans (France)
E-mail: svetlana.eliseeva@cnrs-orleans.fr

[**] This research was supported by a Marie Curie Intra European Fellowship within the 7th European Community Framework Programme, La Ligue Contre le Cancer and La Région Centre. S.P. acknowledges support from the Institut National de la Santé et de la Recherche Médicale. The work in France was carried out in the framework of European Cooperation in Science and Technology Actions TD1004 and CM1006 as well as of Cancéropôle Grand Ouest. We thank David Gosset and the cytometry platform of the Centre de Biophysique Moléculaire for the access to the microscope.

Supporting information for this article is available on the WWW under http://dx.doi.org/10.1002/anie.201311028.

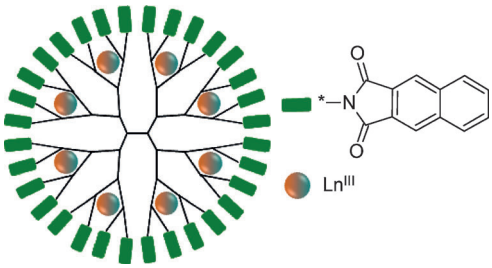

Figure 1. Simplified schematic representation of Ln^{III}-G3P-2,3Nap dendrimer structure.

visible or NIR range maintaining the same intracellular biodistribution and cytotoxicity (Figure 1). Detection in two different ranges of wavelengths is expected to increase the reliability of analysis by reducing risks of artifacts arising from autofluorescence and instrumental errors.

G3P-2,3Nap was synthesized according to a previously developed procedure[11d] starting from amino-terminated generation-3 polyamidoamine dendrimers and 2,3-naphthalic anhydride, and purified by dialysis (See Supporting Information). DMSO solutions of Ln^{III}-G3P-2,3Nap (Ln = Gd or Sm) were prepared by treating the G3P-2,3Nap with eight equivalents of the corresponding Ln^{III} nitrates (Supporting Information). Size distribution analysis of Ln^{III}-G3P-2,3Nap using dynamic light scattering curves confirmed the presence of discrete species with hydrodynamic diameter of 8 ± 2 nm (Figure S1, Supporting Information).

The photophysical properties of (Ln^{III}-)G3P-2,3Nap (Ln^{III} = Sm, Gd) were investigated to evaluate the energy levels of the chromophores. Gd^{III} is a Ln^{III} ion whose emitting energy levels (32000 cm^{-1}) are too high in energy to accept transfer from the chromophore but its incorporation simulates the perturbation imparted by Ln^{III} ions on the electronic structure of the dendrimer. Absorption spectra of Ln^{III}-G3P-2,3Nap and G3P-2,3Nap in DMSO (Figure S2, Supporting Information) have similar profiles and display main bands centered at 290 nm ($\varepsilon \approx 1.8$–2.0×10^5 $M^{-1}cm^{-1}$), 342 nm ($\varepsilon \approx 6.0 \times 10^4$ $M^{-1}cm^{-1}$), and 359 nm ($\varepsilon \approx 8 \times 10^4$ $M^{-1}cm^{-1}$). Upon excitation at 325 nm, Gd^{III}-G3P-2,3Nap exhibits broad-band emission centered at 397 nm (Figure S3, Supporting Information). In time-resolved mode at 77 K, the blue emission is less apparent upon application of a 50 μs time delay after flash and gives rise to a well-structured band with maxima located at 484, 522, and 560 nm and shoulders at 610 and 660 nm which can be assigned to phosphorescence based on their long luminescence lifetimes. These results allow the estimation of positions of the singlet (27280 cm^{-1}, 367 nm) and the triplet (20660 cm^{-1}, 484 nm) states of the dendrimer. It should be noted that the positions of the absorption and emission bands as well as singlet and triplet state energies of (Ln^{III}-)G3P-2,3Nap are similar to those observed for unsubstituted 2,3-naphthalimide,[13] indicating the electronic structure of the chromophoric unit is maintained after attachment to the dendrimer and after Ln^{III} ions have been included. Molar absorption coefficients of (Ln^{III}-)G3P-2,3Nap are high owing to the large number of chromophores attached to the periphery of the dendrimer. Ligand-centered quantum yield of Gd^{III}-G3P-2,3Nap DMSO solution was found to be 1.28(3)% which is 15% higher than the Sm^{III} system, 1.09(4)% (Figure S4, Supporting Information), this loss partially reflects energy transfer from the ligands to the accepting energy levels of Sm^{III} ions. Indeed, Sm^{III}-G3P-2,3Nap upon ligand excitation exhibits sharp emission bands in the visible and in the NIR ranges arising from $^4G_{5/2} \rightarrow {}^6H_J$

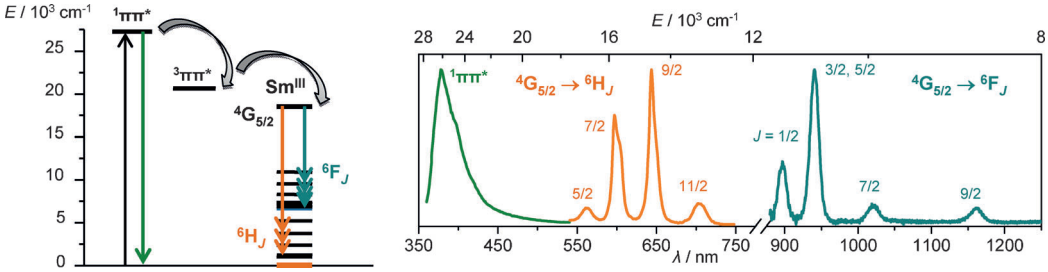

Figure 2. Left: Schematic energy diagram and, right: corrected and normalized emission spectra of the Sm^{III}-G3P-2,3Nap dendrimer under excitation at 325 nm at 298 K (20 μM, DMSO). For the sake of clarity the Sm^{III}-centered emission spectrum in the visible (orange trace) was obtained upon application of a 10 μs delay after flash.

($J = 5/2$–$11/2$) and $^4G_{5/2} \rightarrow {}^6F_J$ ($J = 1/2$–$9/2$) transitions, respectively (Figure 2). Excitation spectra of Sm^{III}-G3P-2,3Nap while monitoring either $^4G_{5/2} \rightarrow {}^6H_{9/2}$ or $^4G_{5/2} \rightarrow {}^6F_{3/2,5/2}$ transitions are similar with a maximum located at approximately 380 nm, corresponding to the ligand absorption spectra (Figure S5, Supporting Information). These results indicate that the Sm^{III} emission originates from an "antenna effect" between the chromophores located on the dendrimer branches and the Sm^{III} ions in the interior.[14] An extension of the excitation band towards longer wavelengths up to 520 nm can be noted which may reflect the possible involvement of the lower-lying energy levels ($n\pi^*$ or additional $^3\pi\pi^*$ states) in the population of the $^4G_{5/2}$ level of the Sm^{III} ion. This feature is advantageous in view of biological applications of Sm^{III}-G3P-2,3Nap since the excitation wavelength can be shifted to more biologically friendly ranges as lower energy excitation typically induces less perturbation in the biological system. Lanthanide-centered quantum yields of Sm^{III}-G3P-2,3Nap DMSO solutions upon 320–340 nm excitation are $2.2(2) \times 10^{-2}$% and $8.5(5) \times 10^{-4}$% for the visible ($^4G_{5/2} \rightarrow {}^6H_J$) and for the NIR ($^4G_{5/2} \rightarrow {}^6F_J$) emission bands, respectively. The luminescence lifetime of the sensitized $^4G_{5/2}$ pathway of Sm^{III}-G3P-2,3Nap DMSO solutions is 15.1(6) μs, which is comparable to values reported for other Sm^{III} complexes.[5a]

To demonstrate the ability of Sm^{III}-G3P-2,3Nap to be used as an imaging agent in living cells, the viability of two cell

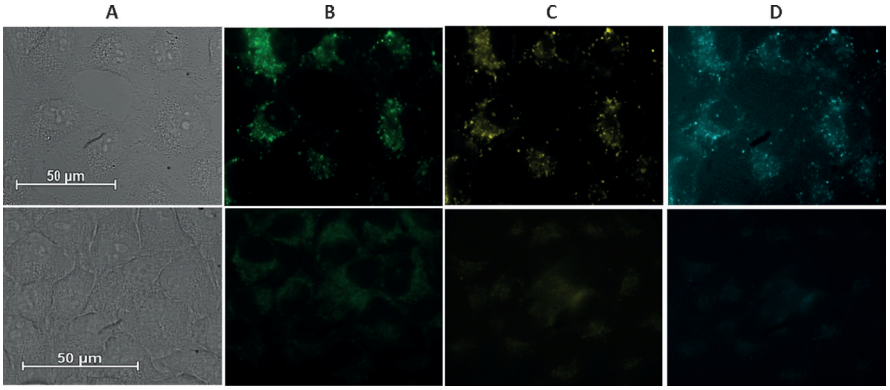

Figure 3. Visible and NIR epifluorescence microscopy on HeLa cells. Top: after incubation with 1 μM Sm^{III}-G3P-2,3Nap and Bottom: untreated cells. A) bright field. B) dendrimer-centered emission (λ_{ex} = 377 nm, band pass 50 nm; λ_{em} = 445 nm, band pass 50 nm; 200 ms of exposition). C) Sm^{III} emission in the visible range (λ_{ex} = 377 nm, band pass 50 nm; λ_{em} = 650 nm, band pass 60 nm; 600 ms of exposition). D) Sm^{III} emission in the NIR range (λ_{ex} = 377 nm, band pass 50 nm; λ_{em} = long-pass filter 770 nm; 5 s of exposition).

lines, HeLa and NIH 3T3, was evaluated by the Alamar Blue assay. Cell viability of 80% for HeLa and 88% for NIH 3T3 cells could be observed after 24 h of incubation with Sm^{III}-G3P-2,3Nap up to a concentration of 2.5 μM (Figure S6, Supporting Information). Therefore, microscopy experiments were performed at 1 μM concentrations of the Sm^{III} probe where cell viability is higher than 95%.

The confocal microscopy images of HeLa cells after incubation with Sm^{III}-G3P-2,3Nap (Figure S7, Supporting Information) under sectioning in the *z*-plane (1 μm optical slice) indicate that the probe was taken up by cells, and the intracellular distribution is consistent with an association between cytoplasmic structures most probably lysosomes.[15] Furthermore, epifluorescence microscopy on HeLa cells (Figure 3) confirmed the ability to detect Sm^{III}-centered signals in the visible (650 nm, band pass 60 nm, filter) and in the NIR (long-pass filter 770 nm) ranges under excitation with 377 nm (band pass 50 nm) filter. In addition, the 2,3-naphthalimide-centered emission (455 nm, band pass 50 nm, filter) could also be observed. Using these experimental conditions, this compound is sufficiently stable in the cell even after 24 h of incubation, allowing detection of the characteristic Sm^{III} emission bands through the energy-transfer processes dictated by the 2,3-naphthalimide moieties.

In summary, we have established as a proof-of-principle that a Sm^{III} macromolecular complex can operate as a bioprobe suitable for microscopy in living cells, emitting both visible and NIR light. This result could be obtained through the relatively high density of photons resulting from the macromolecular structure which combines eight Ln^{III} cations and thirty-two chromophoric sensitizers. Therefore, the effectively low quantum yields recorded for Sm^{III} emission in the visible region is overcome in microscopy experiments, achieving sufficient detection sensitivity to obtain good-quality images of cells with relatively short exposure time. In addition, characteristic NIR Sm^{III} emission has also been used for cellular imaging, representing one of the very few examples of NIR Ln^{III}-based bioprobes.[16] Finally, the versatility of the polyamidoamine dendrimer platform and its straightforward functionalization facilitates further synthetic avenues for improvement by attaching functional groups to increase solubility, control of cellular uptake, localization in a particular organelle, and targeted detection selectivity. These modifications are feasible without necessarily altering the ability of the bioprobe to emit in both visible and NIR domains, therefore maintaining its overall applicability for conventional as well as advanced experimental implementation.

Received: December 19, 2013
Published online: February 3, 2014

Keywords: cytotoxicity · dendrimers · imaging agents · lanthanides · luminescence

[1] H. Kobayashi, M. Ogawa, R. Alford, P. L. Choyke, Y. Urano, *Chem. Rev.* **2010**, *110*, 2620–2640.
[2] L. Yuan, W. Y. Lin, K. B. Zheng, L. W. He, W. M. Huang, *Chem. Soc. Rev.* **2013**, *42*, 622–661.
[3] J.-C. G. Bünzli, *Chem. Rev.* **2010**, *110*, 2729–2755.
[4] J.-C. G. Bünzli, S. V. Eliseeva, in *Springer Series on Fluorescence. Lanthanide Luminescence: Photophysical, Analytical and Biological Aspects*, *Vol. 7* (Eds.: P. Hänninen, H. Härmä), Springer, Berlin, **2011**, pp. 1–45.
[5] a) H. Hakala, P. Liitti, J. Peuralahti, J. Karvinen, V. M. Mukkala, J. Hovinen, *J. Lumin.* **2005**, *113*, 17–26; b) S. Biju, Y. K. Eom, J.-C. G. Bünzli, H. K. Kim, *J. Mater. Chem. C* **2013**, *1*, 6935–6944; c) P. Wang, R. Q. Fan, Y. L. Yang, X. R. Liu, P. Xiao, X. Y. Li, W. Hasi, W. W. Cao, *CrystEngComm* **2013**, *15*, 4489–4506.
[6] Y. Y. Xu, I. Hemmilä, T. Lövgren, *Analyst* **1992**, *117*, 1061–1069.
[7] A.-S. Chauvin, S. Comby, B. Song, C. D. B. Vandevyver, J.-C. G. Bünzli, *Chem. Eur. J.* **2008**, *14*, 1726–1739.
[8] a) E. Buhleier, W. Wehner, F. Vögtle, *Synthesis* **1978**, 155–158; b) C. J. Hawker, J. M. J. Fréchet, *J. Am. Chem. Soc.* **1990**, *112*, 7638–7647; c) G. R. Newkome, Z. Yao, G. R. Baker, V. K. Gupta, *J. Org. Chem.* **1985**, *50*, 2003–2004.
[9] a) S. Svenson, D. A. Tomalia, *Adv. Drug Delivery Rev.* **2012**, *64*, 102–115; b) D. Astruc, E. Boisselier, C. Ornelas, *Chem. Rev.* **2010**, *110*, 1857–1959; c) P. Bhattacharya, N. K. Geitner, S. Sarupria, P. C. Ke, *Phys. Chem. Chem. Phys.* **2013**, *15*, 4477–4490; d) S. M. Grayson, J. M. J. Fréchet, *Chem. Rev.* **2001**, *101*, 3819–3868; e) J. Satija, V. V. R. Sai, S. Mukherji, *J. Mater. Chem.* **2011**, *21*, 14367.
[10] a) S.-T. Lo, A. Kumar, J.-T. Hsieh, X. Sun, *Mol. Pharm.* **2013**, *10*, 793–812; b) S. Sadekar, H. Ghandehari, *Adv. Drug Delivery Rev.* **2012**, *64*, 571–588; c) H. Kobayashi, Y. Koyama, T. Barrett, Y. Hama, C. A. S. Regino, I. S. Shin, B.-S. Jang, N. Le, C. H. Paik, P. L. Choyke, Y. Urano, *ACS Nano* **2007**, *1*, 258–264; d) C. Kojima, B. Turkbey, M. Ogawa, M. Bernardo, C. A. Regino, L. H. Bryant, Jr., P. L. Choyke, K. Kono, H. Kobayashi, *Nanomed. Nanotechnol. Biol. Med.* **2011**, *7*, 1001–1008.
[11] a) Z. S. Pillai, P. Ceroni, M. Kubeil, J. M. Heldt, H. Stephan, G. Bergamini, *Chem. Asian J.* **2013**, *8*, 771–777; b) V. Balzani, P. Ceroni, M. Maestri, V. Vicinelli, *Curr. Opin. Chem. Biol.* **2003**, *7*,

657 – 665; c) Y. Niu, H. Lu, D. Wang, Y. Yue, S. Feng, *J. Organomet. Chem.* **2011**, *696*, 544 – 550; d) J. P. Cross, M. Lauz, P. D. Badger, S. Petoud, *J. Am. Chem. Soc.* **2004**, *126*, 16278 – 16279.

[12] a) M. A. Alcala, S. Y. Kwan, C. M. Shade, M. Lang, H. Uh, M. Wang, S. G. Weber, D. L. Bartlett, S. Petoud, Y. J. Lee, *Nanomed. Nanotechnol. Biol. Med.* **2011**, *7*, 249 – 258; b) M. A. Alcala, C. M. Shade, H. Uh, S. Y. Kwan, M. Bischof, Z. P. Thompson, K. A. Gogick, A. R. Meier, T. G. Strein, D. L. Bartlett, R. A. Modzelewski, Y. J. Lee, S. Petoud, C. K. Brown, *Biomaterials* **2011**, *32*, 9343 – 9352.

[13] V. Wintgens, P. Valat, J. Kossanyi, L. Biczok, A. Demeter, T. Berces, *J. Chem. Soc. Faraday Trans.* **1994**, *90*, 411 – 421.

[14] H. Uh, S. Petoud, *C. R. Chim.* **2010**, *13*, 668 – 680.

[15] A. Saovapakhiran, A. D'Emanuele, D. Attwood, J. Penny, *Bioconjugate Chem.* **2009**, *20*, 693 – 701.

[16] a) A. Foucault-Collet, K. A. Gogick, K. A. White, S. Villette, A. Pallier, G. Collet, C. Kieda, T. Li, S. J. Geib, N. L. Rosi, S. Petoud, *Proc. Natl. Acad. Sci. USA* **2013**, *110*, 17199 – 17204; b) A. D'Aléo, A. Bourdolle, S. Brustlein, T. Fauquier, A. Grichine, A. Duperray, P. L. Baldeck, C. Andraud, S. Brasselet, O. Maury, *Angew. Chem.* **2012**, *124*, 6726 – 6729; *Angew. Chem. Int. Ed.* **2012**, *51*, 6622 – 6625.

